Biochemistry and Biophysics Reports 37 (2024) 101603

Contents lists available at ScienceDirect

Biochemistry and Biophysics Reports

journal homepage: www.elsevier.com/locate/bbrep

Significant role of *PPP3CB* in malignant gliomas development, prognosis and potential therapeutic application—a study based on comprehensive bioinformatics, cell experiments and immunohistochemistry analyses

Bo Li [a,1], Ziyi Yang [b,1], Lulu Li [c], Yongxin Wang [d], Feng Jin [e], Lu Zhang [a], Youjing Zhang [b,*]

[a] Department of Neurosurgery, Affiliated Hospital of Jining Medical University, Jining, Shandong, China
[b] Key Laboratory of Cardiovascular Epidemiology, Department of Epidemiology, Fuwai Hospital, National Center for Cardiovascular Diseases, Chinese Academy of Medical Sciences and Peking Union Medical College, Beijing, 100037, China
[c] Division of Surgical Intensive Care Unit, Cardiac Surgery Department, Fuwai Hospital, National Center for Cardiovascular Diseases, Chinese Academy of Medical Sciences and Peking Union Medical College, Beijing, 100037, China
[d] Department of Neurosurgery, First Affiliated Hospital of Xinjiang Medical University, Urumqi, Xinjiang, China
[e] The Affiliated Qingdao Central Hospital of Qingdao University, The Second Affiliated Hospital of Medical College of Qingdao University, Qingdao, 266042, Shandong, China

ARTICLE INFO

Keywords:
Protein phosphatase 3 catalytic subunit beta (PPP3CB)
Malignant gliomas
Bioinformatics analyses
Cell experiments
Immunohistochemistry

ABSTRACT

Introduction: Malignant gliomas are the most prevalent and fatal types of primary malignant brain tumors with poor prognosis. Protein phosphatase 3 catalytic subunit beta (PPP3CB) is a pivotal constituent of the Ca^{2+}/calmodulin-dependent serine/threonine protein phosphatases and widely expressed in brain. We aimed at identifying whether PPP3CB has potential in being a novel biomarker of malignant gliomas, bringing new insights to clinical management and therapy.

Methods: Transcriptomes and clinical data of Glioblastoma (GBM) and low-grade glioma (LGG) samples were downloaded from TCGA and CGGA. We first explored the expressional and survival features of tumor tissues. Then, PPP3CB-associated genes were identified and their functional pathways were explored through GSEA analyses. Western blotting was conducted to modify PPP3CB expression. Samples of glioma patients and healthy controls were collected and immunohistochemistry (IHC) staining was performed to detect protein level. Further, we carried out an immune infiltration analysis, explored the correlation between PPP3CB and immune checkpoint genes, as well as to assessed the tumor mutation burden (TMB) and tumor microenvironment score (TMEscore) of PPP3CB.

Results: PPP3CB expression in malignant glioma tissues was significantly downregulated and was considered an independent prognostic factor. Several functional pathways were observed through functional pathway analyses. PPP3CB's expression was strongly related to the infiltration of various immune cells and expression of key immune checkpoint genes. PPP3CB expression in high-grade gliomas was significantly lower, affecting glioma cells' proliferation and apoptosis in vitro.

Conclusion: PPP3CB was a potential biomarker for the diagnosis and prognosis of malignant gliomas.

1. Introduction

As the "commander" of human activities, the brain plays a pivotal role in various physiological activities of human beings. Malignant gliomas are the most prevalent and fatal types of primary malignant brain tumors, the annual incidence of which were 5.26 per 100,000 people (17,000 new diagnoses per year) [1]. According to the WHO classification, gliomas were divided into four histological grades based on the extent of undifferentiation, anaplasia, and aggressiveness [2]. Pathologically, glioma was characterized by high degrees of invasive infiltration to surrounding brain tissues, while typically does not metastasize to other organs [3]. Apart from traditional therapeutic interventions such as surgical resection, chemotherapy, and ionizing radiation, molecular-targeted therapy and immunotherapy were merging

* Corresponding author.
E-mail address: zhangyoujing_fuwai@163.com (Y. Zhang).
[1] BL and ZY should be regarded as joint first authors.

https://doi.org/10.1016/j.bbrep.2023.101603
Received 19 October 2023; Received in revised form 28 November 2023; Accepted 4 December 2023

in recent years [4–6]. Nevertheless, the overall survival time of glioblastoma and malignant gliomas remains very poor [1]. Generally, the identifying and verifying novel biomarkers would significantly benefit the diagnosis and prognosis of different severe diseases in patients, and glioma is not an exception [7].

PPP3CB, protein phosphatase 3 catalytic subunit beta (genecards.org), consists of four distinct domains: a catalytic domain, a binding segment for calcineurin B, a segment that interacts with calmodulin, and an autoinhibitory segment [8,9]. It is a pivotal constituent of the Ca^{2+}/calmodulin-dependent serine/threonine protein phosphatases, can regulate physiological activities by dephosphorylating substrate proteins [8]. PPP3CB may play roles in the signaling pathways associated with the development of gliomas. Phosphoprotein phosphatases, including PPP3CB, are known to participate in a range of physiological and pathological processes, including cancer [10]. PPP3CB was found to act as a key regulator of calcium/calcineurin signaling in neurons [25]. Furthermore, PPP3CB is extensively expressed across many tissues especially in brain, assuming a significant role in diverse biological processes and maintaining a close association with a range of diseases [9,11]. PPP3CB expression was proved to be an independent prognostic indicator of neuroblastoma with MYCN amplification [12]. The down-regulation of PPP3CB expression affected resistance to Herceptin in HER2-positive breast cancer patients [13]. A miRNA-mRNA regulatory network showed that PPP3CB was associated with the overall survival of glioblastoma [14]. In addition, PPP3CB inhibited G401 cell migration by regulating the epithelial-to-mesenchymal transition of tumor cells [11]. Previous studies have sparked our curiosity about the potential of PPP3CB as a novel biomarker in malignant gliomas. Nevertheless, a comprehensive investigation into the role of PPP3CB in the development of malignant gliomas has been lacking.

It is crucial searching for novel biomarkers related to gliomas, as the evidence in this regard still remains unclear. This study represents the first attempt to explore the characteristics of PPP3CB expression in malignant gliomas using a combination of bioinformatics analyses and experimental investigations (Fig. 1). The results have provided valuable insights into the potential functions, prognostic value, and molecular mechanisms of PPP3CB, shedding new light on its significance in this context.

2. Methods

2.1. Methods and materials of bioinformatics analyses

2.1.1. Data collecting, cleaning, and integrating

Transcriptome data sets of GBM and LGG patients were searched and downloaded from The Cancer Genome Atlas (TCGA, https://tcga-data.nci.nih.gov/tcga/) [15]. After data cleaning, a total of 703 transcriptome samples were collected, including 529 LGG, 169 GBM, and 5 adjacent healthy brain tissues. Two datasets (DataSet ID: mRNAseq_693 and mRNAseq_325) from the Chinese cohort were downloaded from the Chinese Glioma Genome Atlas (CGGA, http://www.cgga.org.cn/) database [16], including 750 GBM samples after data cleaning. Due to the low number of healthy tissue samples, transcriptome data sets of 1152 healthy brain tissues were also downloaded from Genotype-Tissue Expression (GTEx, https://www.gtexportal.org/home) [17]. Then, the clinical data from TCGA and CGGA mentioned above were obtained and integrated after batching bias correction. Clinical indices were also collected for further analysis including PRS type, histology, grade, age, sex, chemo status, IDH mutation, and 1p19q codeletion. All expression data of the investigated gene (PPP3CB) were extracted and integrated for further exploration.

2.1.2. Differentially expressed analysis of PPP3CB in pan-cancer

GEPIA (Gene Expression Profiling Interactive Analysis, http://gepia.cancer-pku.cn/) was a user-friendly website containing multiple effective tools for the analysis of a tremendous amount of RNA sequencing data, aiming to obtain deeper data mining and a comprehensive understanding of gene functions [18]. In our study, PPP3CB expression in various types of tumors compared with normal samples (pan-cancer analyses) were analyzed separately through matching data from TCGA and GTEx via GEPIA. In addition, transcription data of PPP3CB collected from different projects were integrated, and differentially expressed analyses were performed between malignant glioma samples (GBM and LGG) and healthy tissues.

2.1.3. Survival and prognostic analysis of PPP3CB in GBM

The median value was used as the cut-off point to define the high and

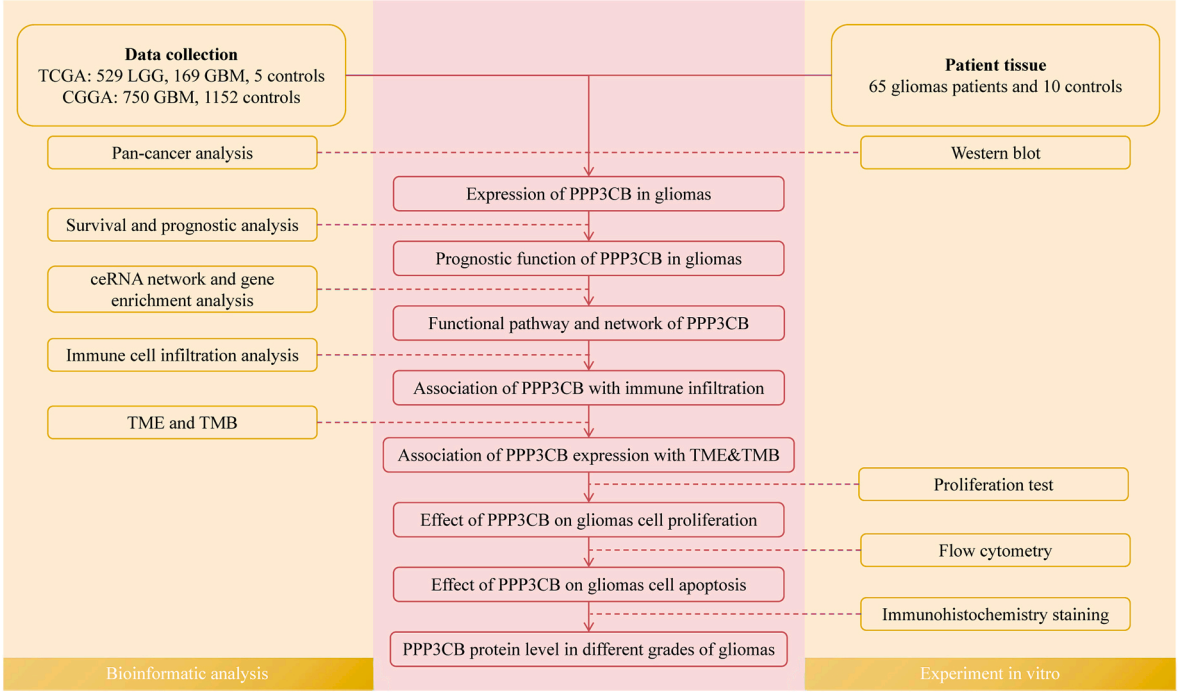

Fig. 1. Workflow of the study.

low expression groups. Survival difference between two expression groups of malignant glioma patients from the TCGA cohort and GBM patients from the CGGA cohort were conducted respectively. After removing incomplete or missing survival data, the survival analysis included 662 patients with TCGA, and 749 patients with CGGA. Univariate and multivariate independent prognostic analyses were performed to identify significant independent prognostic factors, including several clinical characteristics and PPP3CB expressional level, in GBM patients from integrated data. Furthermore, a nomogram was used to predict the prognosis of cancers, estimating the probability of an individual's prognosis by simplifying complex statistic models into a single numerical index [19]. The calibration plot was utilized to validate and assess the reliability of the nomogram [19].

2.1.4. Identification of genes most related to PPP3CB and gene enrichment analysis

PPP3CB-associated genes were selected based on transcriptome data sets from TCGA, the threshold was set as correlation coefficient >0.6 and $P < 0.001$. 11 genes with the strongest associations were screened and their interrelationships were further explored.

Three software programs (miRanda, miRDB, TargetScan) were used to screen miRNAs closely bound to PPP3CB, and the 'Source' database was utilized to identify lncRNAs closely bound to miRNAs. Finally, 'Cytoscape' software was employed for visualization and construction of the ceRNA (Competing endogenous RNA) co-expression network. Moreover, pathway enrichment analyses were performed based on the Kyoto Encyclopedia of Genes and Genomes (KEGG) and the Gene Ontology (GO) term databases. For the GO database, terms of biological processes (BP), molecular functions (MF), and cellular components (CC) were respectively assessed. Gene Set Enrichment Analysis (GSEA) is a powerful analytical method for interpreting gene expression data and revealing enriched biological pathways [20]. Signaling pathways of high interest were identified and their roles in glioma were discussed. The R packages "org.Hs.eg.db" and "clusterProfiler" were utilized for analyses in this step.

2.1.5. Immune cell infiltration analysis, tumor microenvironment (TME) and tumor mutation burden (TMB)

The "Cell type Identification By Estimating Relative Subsets Of RNA Transcripts (CIBERSORT)" algorithm was a large-scale analytic tool for identifying cellular biomarkers and therapeutic targets from bulk RNA-seq data sets, especially used for immune cell infiltration analyses [20,21]. For each sample, inferred fractions of immune cell populations were calculated and applied for further immune analyses. In our study, the infiltration of various immune cells was assessed by this algorithm, then the correlation and difference between the expression level of PPP3CB and the infiltration of immune cells were evaluated. In addition, correlations between immune checkpoint genes and PPP3CB were also assessed. Tumor microenvironment (TME) and tumor mutation burden (TMB) were proven to significantly affect immune infiltration and immune therapy outcomes [22,23], therefore, we assessed association of PPP3CB expression and levels of TME, TMB. During immune-related analyses, the microenvironment score of each subject was obtained by using the R package 'estimate', And then the PPP3CB expression level and the three types of tumor microenvironment scores were integratively analyzed. Mutation data were downloaded from the TCGA database and its possible correlation with PPP3CB was explored after data cleaning and integration.

2.2. Methods and materials of cell experiments

2.2.1. Clinical characteristics of patients and healthy control

The use of glioma patient tissue specimens was acquired from patients as follows: a total of 65 patients with glioma (25 of WHO grade 4, 20 of WHO grade 3, 20 of WHO grade 2) and 10 control healthy tissues were collected from the Affiliated Hospital of Jining Medical University from July 2020 to July 2022. Also, medical records, imaging examinations, pathological sections, wax blocks, and clinicopathological data were recorded. This experiment was approved by the Ethics Committee of Jining Medical University.

2.2.2. GBM cell culture

GBM Cell line U251 was purchased from Wuhan Punuosei Biological Company, LTD.

The cells were cultured in a controlled environment using DMEM (Dulbecco's Modified Eagle Medium) supplemented with 10% newborn bovine serum and 100 U/mL penicillin along with 100 μg/mL streptomycin. The culture was maintained in a 5% CO2 incubator, ensuring saturated humidity and a constant temperature of 37 °C.

2.2.3. Construction and transfection of lentiviral vectors

To investigate PPP3CB's function in glioblastoma cell lines, we performed gene overexpression and interference assay on U251 cells. All experimental steps were carried out according to the instructions. For transfection, 40 μL of lentiviral infection preparation A solution and 40 μL of P solution (comprising HitransG A infection enhancer 25 × and HitransG P infection enhancement solution 25 ×) were added separately to 1.5 ml enzymatic EP tubes. The genetic sequences used in the transfection process were as follows: gene sequence1 5′-CCCGGAAAGAAATCATAAGAAGC-3′, gene sequence1 2 5′-GTCACAATACAGTTCGAGGATGC-3′, and gene sequence1 3 5′-CCTGCTAATACACGATACCTTGC-3'. The cells were transfected with lentivirus and screened with puromycin to construct stable interfered /overexpressed PPP3CB cell lines for further experiments.

2.2.4. Gel electrophoresis and western blotting

In order to assess the transfection efficiency and regulated expression levels of PPP3CB, we conducted western blot experiments on the gene-modified cell lines. Total protein from both tumor cells and tissues was extracted using SDS Lysis Buffer.

The transfected U251 cells were treated with trypsin and subsequently collected by centrifugation. Next, 100 μl of RIPA buffer containing 1 mM PMSF was added to the cells in a 1.5 ml EP tube. The tube was then placed on ice for 20 min, shaken and mixed, followed by an additional 10 min on ice. The resulting suspension was centrifuged at 12000G and 4 °C for 15 min to obtain the protein supernatant. For the tissue samples, a 30 mg specimen was excised from frozen glioma tissue blocks of different grades stored in liquid nitrogen and added to a separate 1.5 ml EP tube. Subsequently, 300 μl of RIPA buffer containing 1 mM PMSF was added, and the tissue was thoroughly homogenized using a high-throughput tissue grinder. The resulting suspension was then transferred to a 1.5 ml EP tube and placed on ice for 30 min. Next, the suspension was centrifuged at 12000G and 4 °C for 15 min to isolate the protein supernatant. The protein content was determined using the BCA method, and the denatured protein was prepared at a high temperature. Equal amounts of protein were then subjected to electrophoresis on 10% SDS gels and subsequently transferred to PVDF membranes. To block non-specific binding, the PVDF membrane was sealed with skimmed milk powder at room temperature for 60 min. Antibodies against PPP3CB (diluted at 1:1000) and anti-beta-actin (diluted at 1:1000) were used for immunoblotting. Following the addition of the primary antibodies, the suspension was incubated overnight at 4 °C to facilitate the antibody-protein interaction. The membrane was incubated with horseradish peroxidase-conjugated goat anti-rabbit IgG (diluted at 1:5000). For Western blot detection, the ECL chemiluminescence kit was employed. The software ImageJ was utilized for precise quantification of the blotting areas, enabling us to obtain the relative protein expression levels for analysis.

2.2.5. CCK-8 proliferation test

The U251 cell culture solution underwent centrifugation, and the resulting cell precipitate was collected, serving as the control group.

Each group was prepared with five wells in a 96-well plate, and 5 × 103 cells were inoculated into each well. To create a perimeter blank, 200 μl of PBS buffer was added around the sample wells in the 96-well plate. The experiment was conducted at 24h, 48h, and 72h time points. After each designated time point, the 96-well plate was retrieved, and the culture medium was discarded. Subsequently, 100 μl of DMEM high sugar medium and 10 μl of CCK-8 were added to each well. Following a 2-h incubation period in the incubator, the 96-well plate was analyzed using a microplate reader to measure the OD value at a wavelength of 490 nm. Statistical results were obtained by 'Group Analyses-Two-way ANOVA' in GraphPad Prism.

2.2.6. Flow cytometry assay for cell apoptosis

The apoptosis rate can be calculated as UR + LR. The U251 cells were subjected to centrifugation and then re-suspended to achieve a concentration of 1-5 × 10^5 cells. After re-suspension using 100 μl of 1 × Binding Buffer, 5 μl of Annexin V-APC and 5 μl of 7-AAD Staining Solution were added to the cells. The cell staining was carried out in darkness at 20–25 °C for 10 min, followed by mixing with 400 μl of Binding Buffer. The samples were analyzed using a DxFLEX flow cytometer, where 10,000 events were collected for each sample. The APC fluorescence is detected in the APC channel and the 7-AAD fluorescence is detected in the PC5.5 channel. Results were further analyzed by the software CytExpert. Cell lines were grouped as follows: (A) interference group, LV-PPP3CB-RNAi, shRNA; (B) control group; (C) overexpression group, LV-PPP3CB.

2.2.7. Immunohistochemistry staining of PPP3CB protein in tissues

We selected 65 tumor tissues of glioma patients with different grades and 10 normal brain tissues for the experiment. Tissues were donated by GBM patients who attended Jinan First Hospital and have signed informed consent. All specimens have been embarrassed, dehydrated, embedded in a 4% neutral formaldehyde solution, and sliced into 3–4 μm thickness cuts. Immunohistochemical staining was performed using the two-step EnVision method. All operations were performed according to the standard procedure of the kit. PPP3CB monoclonal antibody was used as a primary antibody with a dilution concentration of 1:200. Immunohistochemical results were determined by a semi-quantitative scoring of the immunoreactive score (IRS):

$$IRS = SI \times PP,$$

where SI stands for the staining intensity and PP stands for the positive percentage.

The score of positive cell number: 200 cells were counted in each field, a total of 5 positive cells in the high-magnification field (x 200). The percentage of positive cells ≤10% was defined as 1 point, 11%–50% as 2 points, 51%–75% as 3 points, and 75% as 4 points. The grading of staining intensity score: Uncolored (0 points), light yellow (1 point), brownish yellow (2 points), and tan (3 points). The interpretation of IRS: 0–3 as negative (1), 4–6 as weak positive (+), 8–9 as moderate positive (++), and 12 as strongly positive (+++).

2.3. Statistical analyses

Statistical analyses were performed by the R language (version 4.1.1). All downloaded data sets were processed and integrated by the Perl language (strawberry version). Survival analyses of patients from multiple databases were conducted using the Kaplan–Meier method. Non-normally or normally distributed variables were analyzed through the Wilcoxon Test and the unpaired student's t-test, respectively. The Pearson correlation was calculated for the correlation tests. Statistical analysis was performed using GraphPad Prism 7 software (GraphPad Software) for cell experiments. Statistical significance was set at $P < 0.05$ or $P < 0.01$ or $P < 0.0001$.

3. Results

3.1. PPP3CB expression pattern in tumor and normal samples

The results of the pan-cancer analysis revealed that compared to healthy tissues, PPP3CB expression varies in nine types of tumor tissues, which showed lower expression in bladder urothelial carcinoma, cervical squamous cell carcinoma and endocervical adenocarcinoma, GBM, ovarian serous cystadenocarcinoma and rectum adenocarcinoma, as well as showed higher expression in lymphoid neoplasm diffuse large B-cell lymphoma, pancreatic adenocarcinoma and thymoma. (Fig. 2A). After integrating transcription data of PPP3CB in GBM as well as LGG, the expression levels between tumor and normal tissues presented significant differences. Compared with malignant glioma tissues, PPP3CB expression was significantly higher in normal tissues (Fig. 2B). After verification, results showed that the transfection was successful, and the expression of PPP3CB was found to vary significantly across different tissues, with its highest levels observed in normal brain tissues, and conversely, its lowest expression detected in GBM tissues. (Fig. 2 C-D).

3.2. PPP3CB showed significant prognostic potential

The survival analysis demonstrated that higher PPP3CB expression was correlated with better prognosis in both malignant glioma patients ($P < 0.001$, Fig. 3A) and GBM patients ($P < 0.001$, Fig. 3B). Univariate and multivariate independent prognostic analyses revealed that PPP3CB expression (both $P < 0.001$) was an independent prognostic factor (Fig. 3C–D). PPP3CB showed significant affection to the prognosis of GBM patients, and its upregulated expression might work as a beneficial factor (HR < 1).

The nomogram demonstrated the possibility of individualized scoring of patients that could predict their prognosis, optimize clinical intervention, and improve the prognosis of tumor patients (Fig. 4A). In addition, the calibration validated the stability and reliability of the nomogram (Fig. 4B). Consequently, PPP3CB appeared to be a strong prognosticator in GBM patients.

3.3. Identification of PPP3CB-associated network and results of gene enrichment analyses

Genes associated with PPP3CB were identified, and six genes with the strongest positive correlation as well as five genes with the strongest negative correlation were screened out (Fig. 5A–K). Subsequently, the correlation between PPP3CB and these 11 genes was explored, as shown in Fig. 5L. Furthermore, the ceRNA network was shown in Fig. 6A, suggesting the complex regulatory network established between PPP3CB expression and different types of RNA. GSEA analysis revealed that the differential expression of PPP3CB was associated with the regulation of multiple functional pathways, including the calcium signaling pathway, cytokine-cytokine receptor interaction, and long-term potentiation (KEGG, Fig. 6B), as well as the adaptive immune response based on somatic recombination of immune receptors built from immunoglobulin superfamily domains, B cell-mediated immunity, and calcium ion regulated exocytosis (GO, Fig. 6C).

A heatmap of the 30 most significantly differentially expressed genes between malignant gliomas and normal samples were presented in Fig. 6D. Through GO pathway analyses (Fig. 6E), differentially expressed genes were mainly enriched in signal release, extracellular matrix organization, and extracellular structure organization (BP); collagen-containing extracellular matrix, presynapse and synaptic membrane (CC); passive transmembrane transporter activity (MF). In Fig. 6F, KEGG analyses demonstrated that genes were mainly enriched in neuroactive ligand-receptor interaction, cytokine−cytokine receptor interaction, and systemic lupus erythematosus.

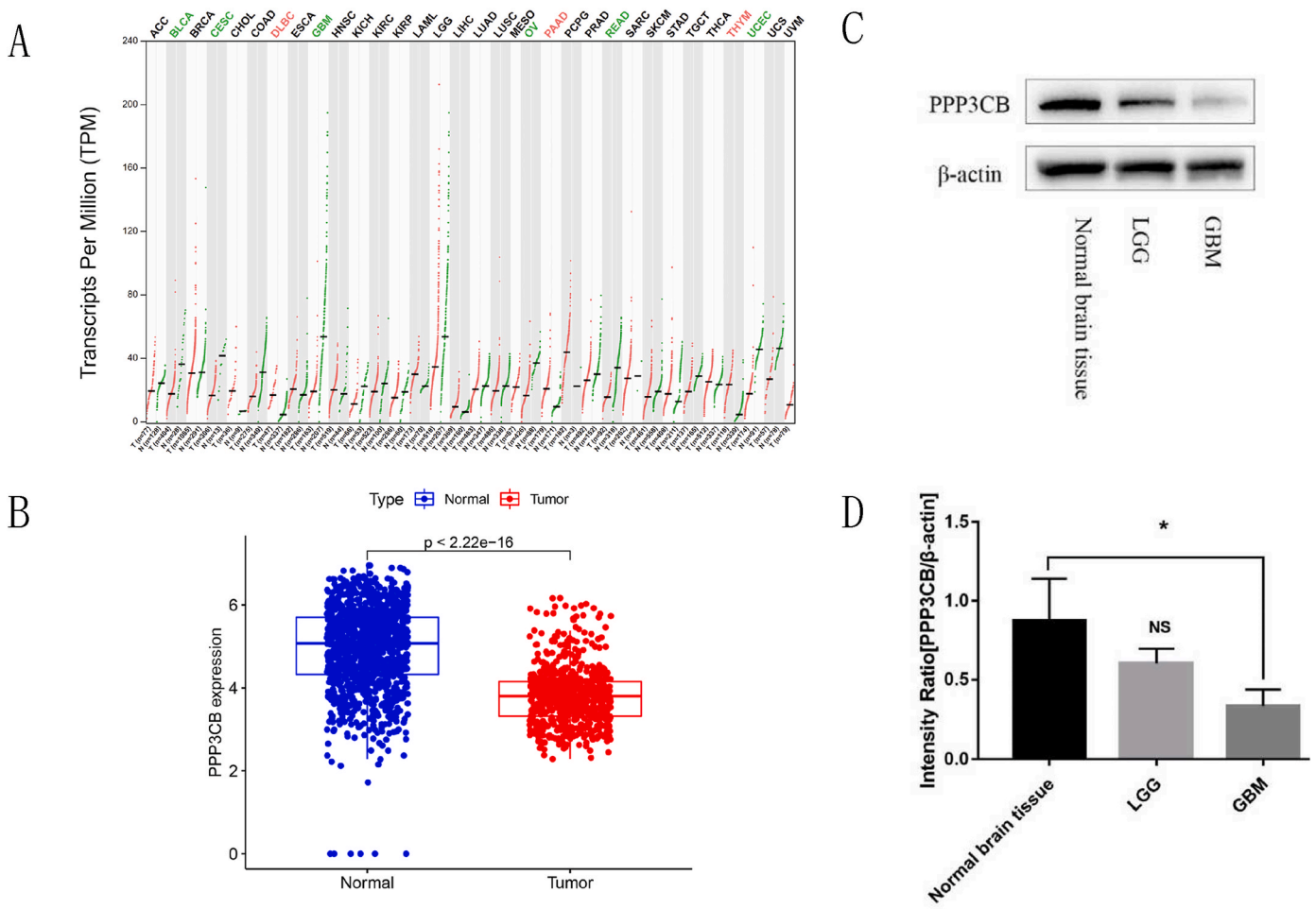

Fig. 2. A: Results of pan-cancer analyses. PPP3CB showed lower expression in tumors colored in the green font (BLCA: Bladder Urothelial Carcinoma, CESC: Cervical squamous cell carcinoma and endocervical adenocarcinoma, GBM: Glioblastoma multiforme, OV: Ovarian serous cystadenocarcinoma, READ: Rectum adenocarcinoma, UCEC: Uterine Corpus Endometrial Carcinoma), and higher expression in tumors colored in the red font (DLBC: Lymphoid Neoplasm Diffuse Large B-cell Lymphoma, PAAD: Pancreatic adenocarcinoma, THYM: Thymoma). B: PPP3CB's expression in malignant gliomas and tumor patients. C–D: Expressional levels of PPP3CB in normal brain tissue, low-grade glioma tissue (LGG), and high-grade glioma tissue (GBM). *P* values were determined by ANOVA with multiple comparison test. *: $P < 0.05$, ns: not significant. (For interpretation of the references to color in this figure legend, the reader is referred to the Web version of this article.)

3.4. PPP3CB expression was strongly associated with the infiltration of immune cells and the immune checkpoint genes

Between the high and low expression groups of PPP3CB, we identified 22 immune cells with significantly different infiltration levels (Fig. 7A). PPP3CB expression presented a significant correlation with the infiltration of 13 types of immune cells ($P < 0.05$), including 7 kinds of negative correlation and 6 kinds of positive correlation (Fig. 7B). Accumulated macrophages whereas decreased M0 macrophages were observed in PPP3CB-enriched tumors. In addition, PPP3CB expression showed a strong correlation with several immune checkpoint genes, positively or negatively (Fig. 7C). TMB has been extensively studied in various solid tumors, as it has the potential to serve as a crucial indicator of therapeutic responsiveness to immunotherapy such as immune checkpoint inhibitors. PPP3CB was significantly inversely associated with tumor mutational burden (Fig. 8B). TMEscore has also been proven to be a predictive biomarker of response to checkpoint immunotherapy in various cancers [24]. There were significant differences between the high and low expression groups of PPP3CB in the three types of tumor microenvironment scores ($P < 0.001$, Fig. 8A). In summary, PPP3CB could potentially influence the therapeutic outcomes.

3.5. Upregulation of PPP3CB could inhibit glioma cell proliferation

As shown in Fig. 9, the proliferation rate of glioma cells gradually increases with time, and there was a big difference between the experimental group and the control group ($P < 0.0001$). Among them, the low-expression PPP3CB group had the highest proliferation rate at the three testing times, while the over-expression PPP3CB group had a significantly lower proliferation rate than the control group and the low-expression PPP3CB group. Overall, the results demonstrated that glioma proliferation was inhibited with the increase of PPP3CB gene expression, indicating PPP3CB's affection for the proliferation of GBM U251 cell lines.

3.6. Upregulated PPP3CB expression promoted glioma cell apoptosis

Flow cytometry was performed to further investigate the correlation between PPP3CB expression and apoptosis in vitro. Results of flow cytometry were shown in Fig. 10, LL was the lower left (normal negative control cells), UL was the upper left (fragmented and damaged cells), UR was the upper right (late apoptotic and dead cells), and LR was the lower right (early apoptotic cells). Compared with the control group, interference with PPP3CB expression inhibited apoptosis of U251 cells, while its overexpression promoted apoptosis (the apoptosis rate of the control group was 17.26 ± 2.48%, the interference group was 7.13 ± 2.53%,

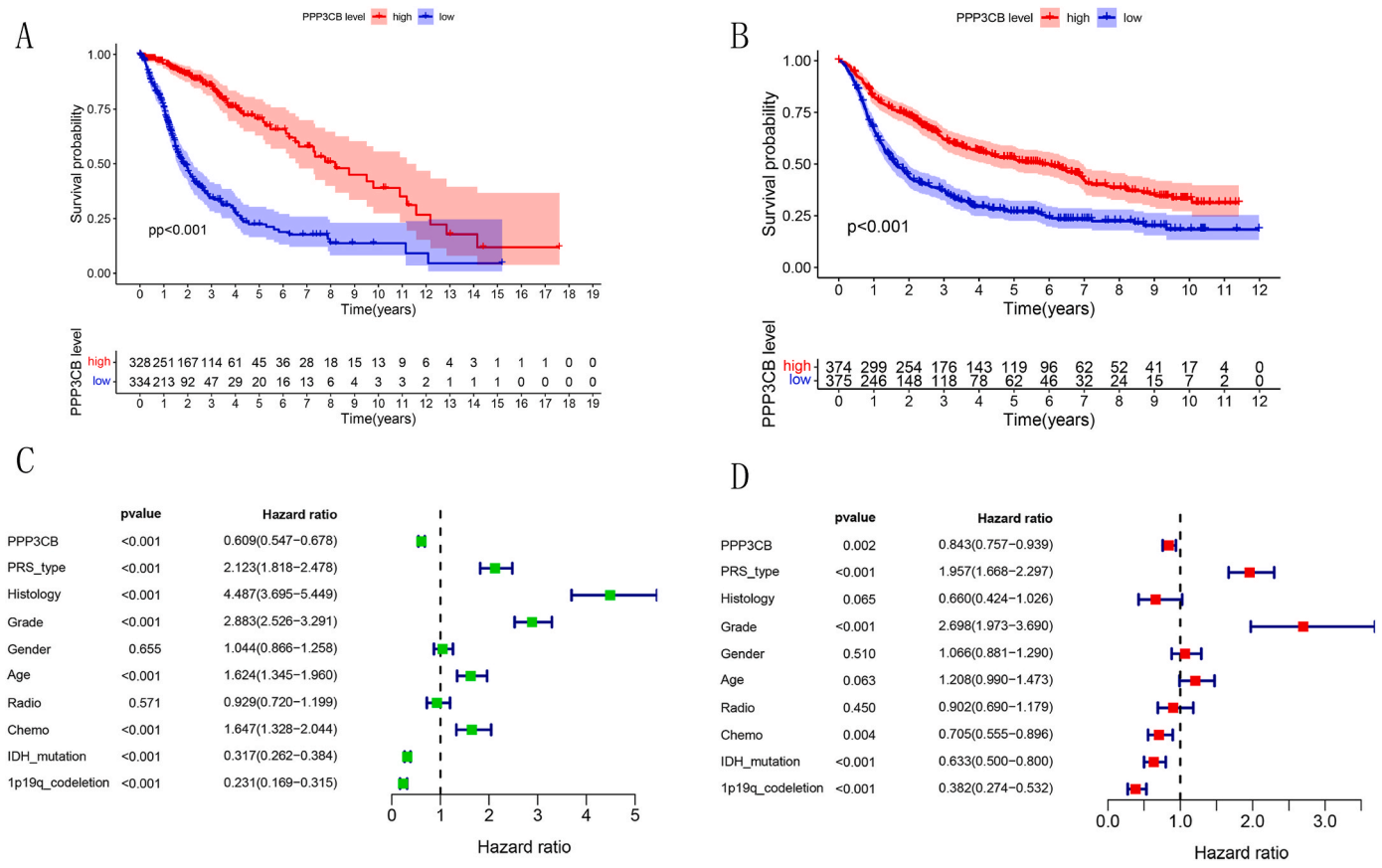

Fig. 3. A: Survival analyses of malignant gliomas from TCGA. B: Survival analyses of GBM from CGGA. C: Univariate independent prognostic analyses of GBM patients from CGGA. D: Multivariate independent prognostic analyses of GBM patients from CGGA.

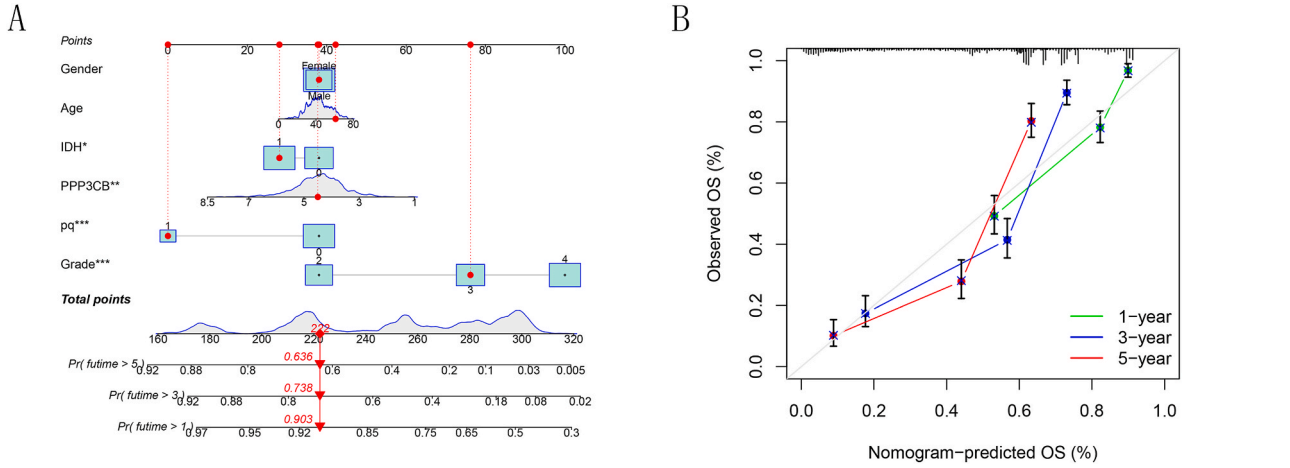

Fig. 4. A: The nomogram comprising both clinical factors and PPP3CB expression. B: Calibration curves for 1-, 3-, and 5-year OS rates in the established nomogram.

and the overexpression group was 26.53 ± 6.53%). The statistical analysis showed that the interference group and the overexpression group had a significant statistical difference ($P < 0.01$). PPP3CB may promote apoptosis of glioma and play an anti-tumor role.

3.7. Immunohistochemical staining of PPP3CB expression

The in vitro experiment results preliminarily showed that PPP3CB expression was closely related to the proliferation and apoptosis of glioma cell lines. To depict the role of PPP3CB in glioma more accurately, we selected a batch of glioma patient specimens for immunohistochemical staining. The clinical characteristics of patients were presented in Table 1. Fig. 11 showed representative immunohistochemical staining results and scores, significantly low protein expression levels were observed in tumor tissues (Fig. 11A–D). Through Wilcoxon symbolic rank test, different grades of gliomas had highly different protein expression levels, which were also shown in Table 1.

4. Discussion

PPP3CB is a key protein of the Ca^{2+}/calmodulin-dependent serine/threonine protein phosphatases and plays important roles in various

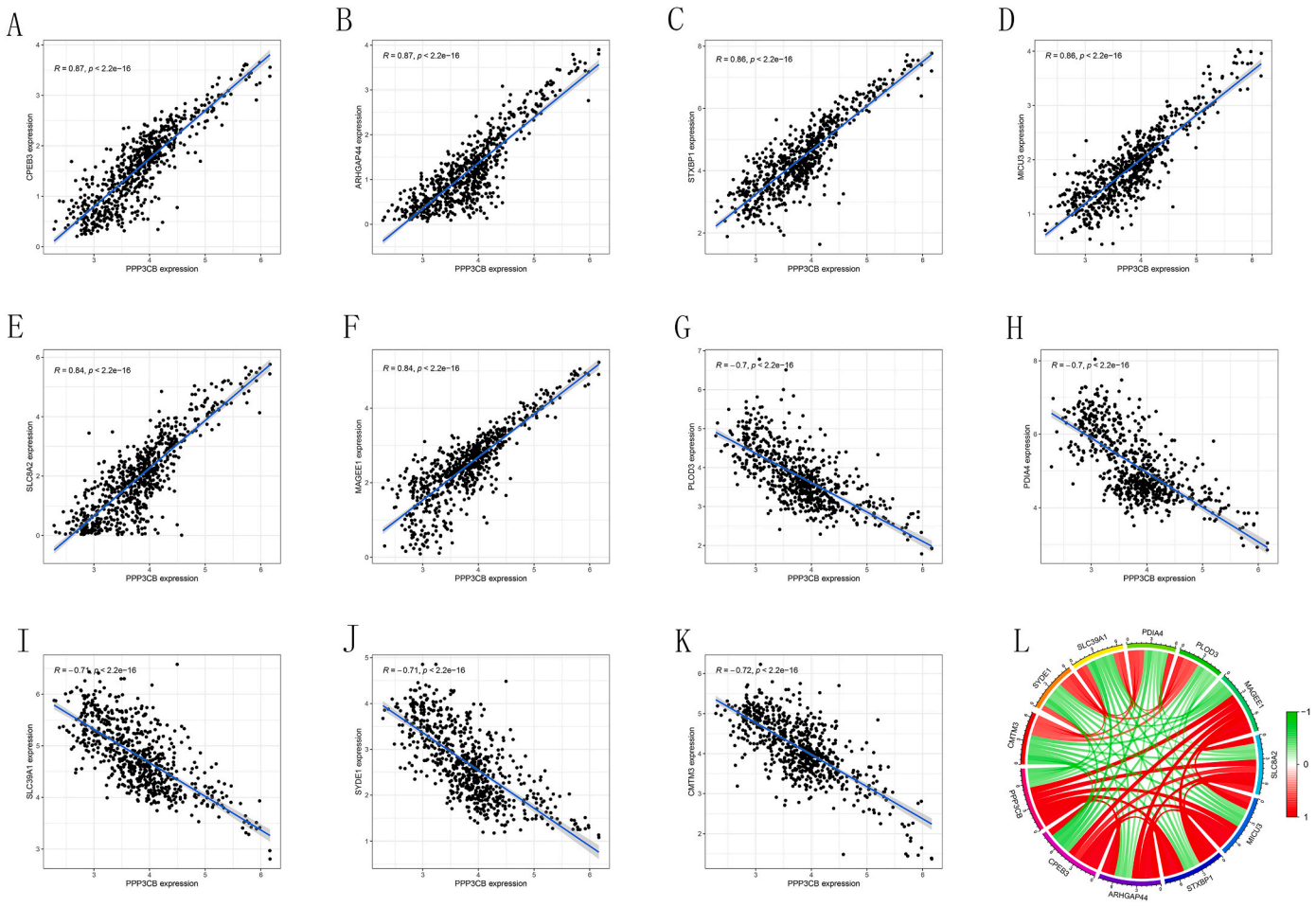

Fig. 5. A–K: Scatter plots of 11 PPP3CB-associated genes. L: A circle diagram presenting the correlation between PPP3CB and these eleven genes.

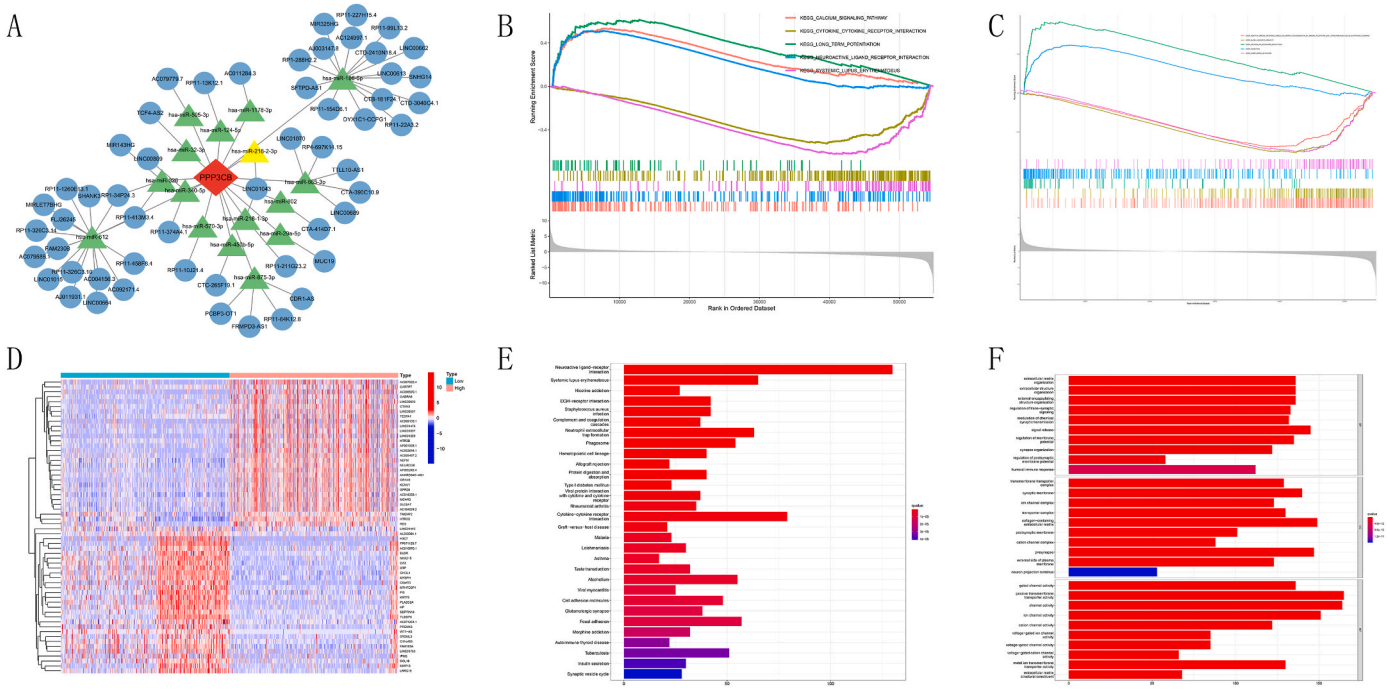

Fig. 6. A: the ceRNA network of PPP3CB B: Results of GSEA analyses (KEGG). C: Results of GSEA analyses (GO). D: A heatmap of the 30 most significantly differentially expressed genes between malignant gliomas and normal samples. E: A histogram showing the results of GO analyses F: A histogram showing the results of KEGG analyses.

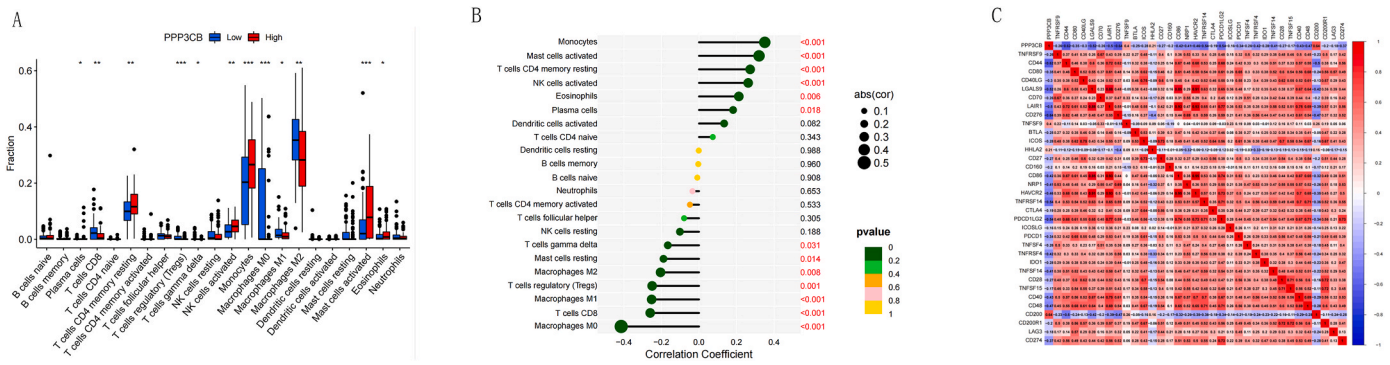

Fig. 7. A: Immune cell infiltration differences between the high and low-expression groups of PPP3CB. B: Correlation between immune cell infiltration and PPP3CB expression. C: Correlation between PPP3CB and immune checkpoint genes.

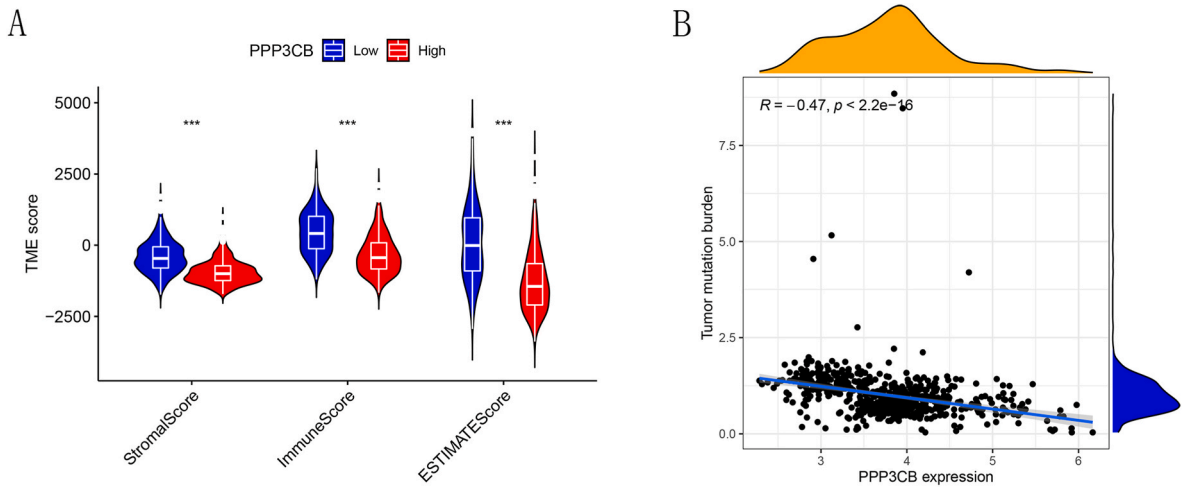

Fig. 8. A: Three types of tumor microenvironment scores differed in two PPP3CB expressional groups. B: Correlation between tumor mutation burden and PPP3CB expression.

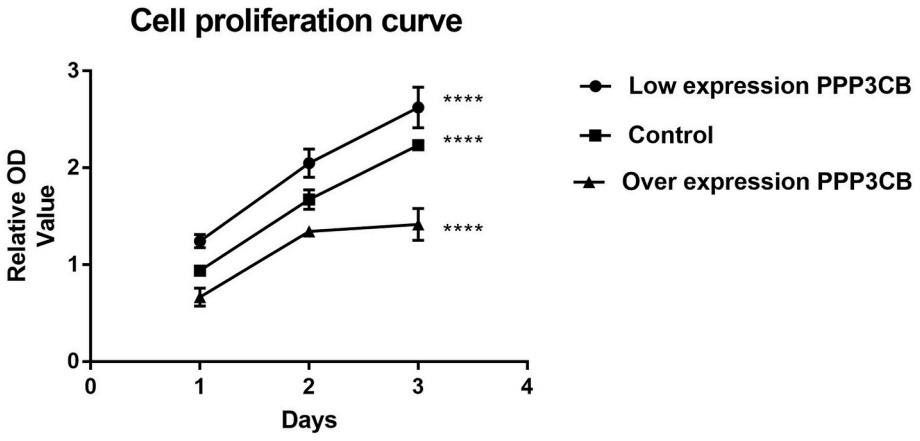

Fig. 9. Association between PPP3CB expression and proliferation of glioma cells. *P* values were determined by ANOVA with multiple comparison test. ****: $P < 0.0001$.

types of tumors, its impacts on the development of brain tumors, and malignant gliomas (GBM and LGG) remained unclear. Through bioinformatics analyses and in vitro experiments, our study made a comprehensive exploration of the characteristics of PPP3CB's expression and its correlation with patient prognosis, immune infiltration, protein level as well as cell proliferation and apoptosis status in malignant gliomas. Our research provides important clues and evidence for a comprehensive analysis of the role of PPP3CB in the occurrence and development of gliomas, offering new potential insights for the prognosis identification and management of malignant glioma patients.

Huang et al. concluded that phosphoprotein phosphatases (PPPs) were significantly associated with the prognosis of pancreatic cancer, similar to our results in malignant gliomas [25]. Bioinformatics and Western-Blot analyses concluded that, compared with healthy samples

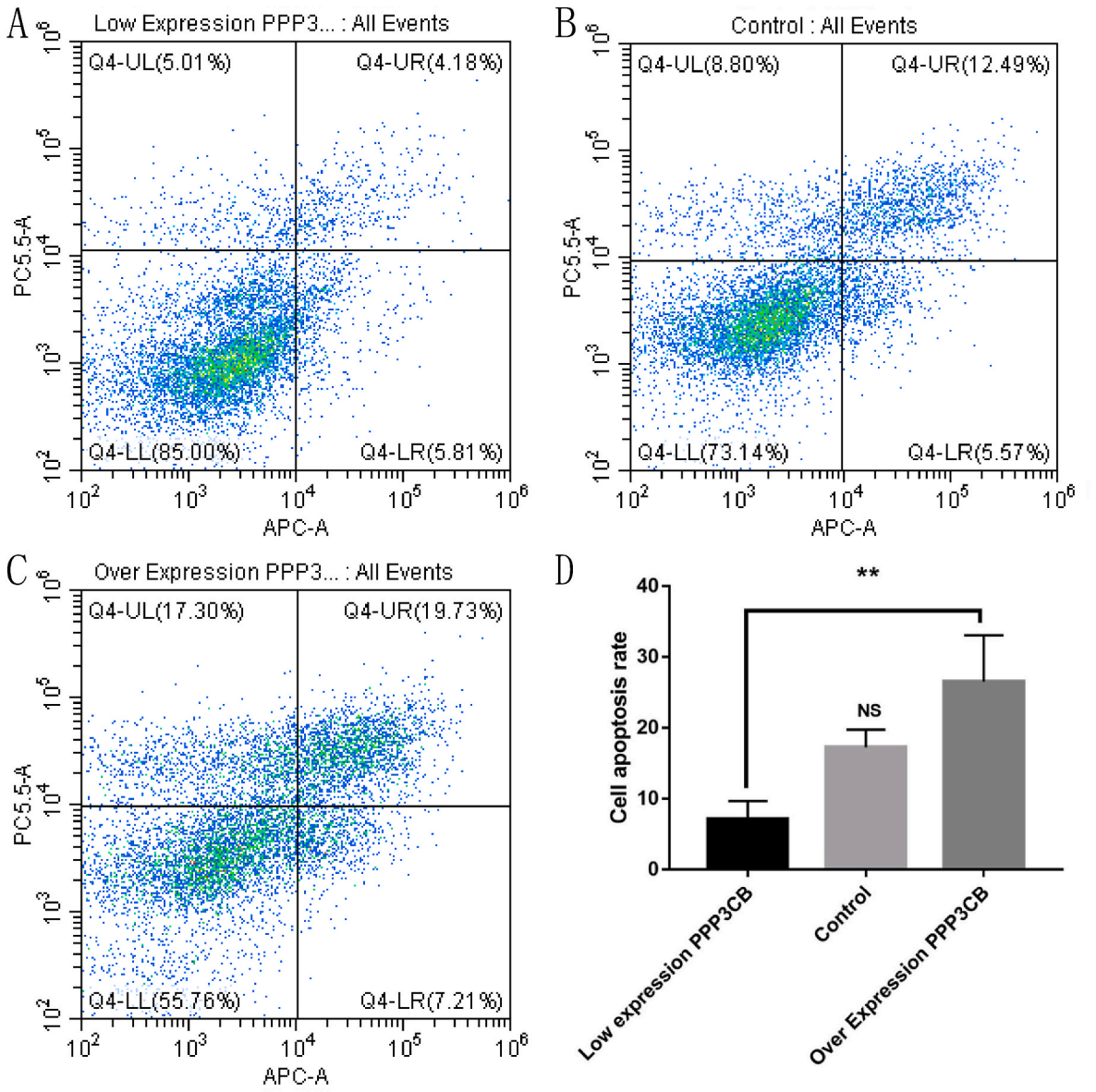

Fig. 10. The flow cytometry results. Q4-UL was the upper left (fragmented and damaged cells), Q4-UR: was the upper right (late apoptotic and dead cells), Q4-LL: was the lower left (normal negative control cells), Q4-LR was the lower right (early apoptotic cells). A: The correlation between PPP3CB expression and apoptosis in vitro of low expression group. B: The correlation between PPP3CB expression and apoptosis in vitro of the control group. C: The correlation between PPP3CB expression and apoptosis in vitro of the overexpression group. D: Histogram of cell apoptosis in three groups. *P* values were determined by ANOVA with multiple comparison test. **: $P < 0.01$, ns: not significant.

Table 1
Clinical characteristics of 65 glioma and 10 control patients.

		WHO grade 4	WHO grade 3	WHO grade 2	Control group	Total
Age	≥65	6	3	3	0	12
	<65	19	17	17	10	63
Sex	Male	15	11	12	9	47
	Female	10	9	8	1	28
Pathological type	astrocytoma	0	6	8	0	14
	Oligodendroglioma	0	3	4	0	7
	glioblastoma	23	0	0	0	23
	Anaplastic astrocytoma	0	10	0	0	10
	Other types	2	1	8	0	11
	gliosis	0	0	0	10	10
PPP3CB expression scores	3+	0	0	0	10	10
	2+	0	0	20	0	20
	1+	0	20	0	0	20
	0	25	0	0	0	25
Total		25	20	20	10	75

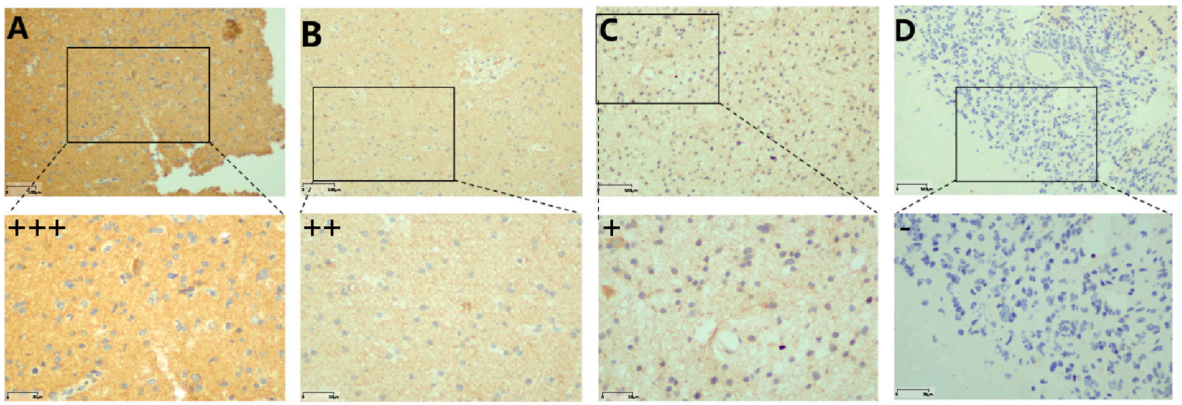

Fig. 11. Results of immunohistochemical staining. A: High expression staining of PPP3CB in normal and glioma brain tissue. B: Medium expression staining of PPP3CB in normal and glioma brain tissue. C: Low expression staining of PPP3CB in normal and glioma brain tissue. D: Representative negative expression staining of PPP3CB in normal and glioma brain tissue.

and low-grade gliomas, a lower expression level of PPP3CB was detected in high-grade malignant gliomas, and the decrease in PPP3CB expression indicates a poor prognosis. Additionally, higher PPP3CB expression acted as an independent beneficial prognostic feature in GBM patients. The personal scores calculated from the nomogram could be applied for clinical management and prognostic prediction.

Nolze et al. found that the macroautophagy/autophagy in neuron counteracts might be regulated by calcium-dependent phosphatase PPP3/calcineurin activation and therefore affected the prognosis of neurodegenerative diseases [26]. Similarly, another study revealed that PPP3CB was a key regulator of calcium/calcineurin signaling [27]. A higher expression of PPP3CB was one of the potential biomarkers for schizophrenia patients [28].

We identified genes closely associated with PPP3CB and conducted pathway analysis. Functional pathway analyses of our study drew similar conclusions, indicating calcium signaling pathway presented great potential for diagnosis and prognosis of malignant gliomas. Relevant miRNAs and LncRNAs were identified and a ceRNA co-expression network was constructed, highlighting key RNAs that may require further investigation in the future.

Furthermore, PPP3CB expression was strongly related to the infiltration of several immune cells and immune checkpoint genes. Recent evidence indicates that suppression of calcineurin signaling and its influence on the immune system could enhance cancer stem cell potential [29]. Immune checkpoint inhibitors (ICPs) have been progressively integrated into clinical practice. However, the responsiveness and resistance are influenced by various factors, including the tumor microenvironment, TMB, and TME. Study on tumors' escaping from immunosurveillance has received extensive attention in recent years, which demonstrated the broad prospects of immunotherapy in the treatment of GBM and further exploration was needed in the future [4]. Results showed higher expression of PPP3CB indicated lower TMB, although current research indicates that a high TMB is beneficial for immunotherapy and leads to a higher patient survival rate, the impact of TMB varies considerably among distinct types of cancer [30]. Matten et al. showed that low mutation burden is associated with longer survival after virotherapy in glioblastoma patients [31]. Moreover, the tumor microenvironment significantly affected the occurrence and development of tumors, thereby influencing the clinical status and prognosis of the patient. TMEscore has been proven to be a predictive biomarker of response to checkpoint immunotherapy in many cancers [24].PPP3CB showed significant differences in three types of TMEscores, suggesting that the level of PPP3CB could potentially influence therapeutic outcomes. Chen et al. found that chemokine in the tumor microenvironment would promote microglia infiltration and may be regarded as a novel therapeutic target in GBM [32]. PPP3CB profoundly influenced tumor immunity and may serve as a crucial weapon in the future development of novel tumor immunotherapies.

Through cell cycle determination, we found low expression of PPP3CB could promote the proliferation of glioma cells, indicating higher malignancy and a greater level of damage. Downregulated PPP3CB expression might inhibit the apoptosis of glioma cells. Interestingly, previous study suggests that apoptotic GBM cells secrete spliceosome-enriched extracellular vesicles that promote tumor cell proliferation and resistance to therapy [33]. More GBM cell lines should be included in cell experiments to explore the biological functions of PPP3CB. PPP3CB had great potential of being a novel biomarker and would contribute to the further understanding of malignant gliomas.

There were some limitations in our study. Since our research contained few wet-lab experiments and the specific mechanism involving how PPP3CB affected malignant gliomas remained unveiled, more in-depth studies were required. Furthermore, a prospective cohort study is needed to validate our conclusion about PPP3CB's prognosis potential. Finally, the biological functions of PPP3CB in other types of GBM cell lines should be further explored.

5. Conclusion

In conclusion, PPP3CB was identified as a potentially significant biomarker for the diagnosis and prognosis of malignant gliomas, its impacts on glioma might be associated with the regulation of the calcium signaling pathway. Our study brought valuable insights into improving clinical management and provided a more comprehensive understanding of malignant gliomas. The mechanism of PPP3CB needs to be investigated in animal models, and further research should explore the functions of PPP3CB in other types of GBM cell lines.

Ethics approval

All work described has been carried out in accordance with The Code of Ethics of the World Medical Association (Declaration of Helsinki) for experiments involving humans. The study was approved by the Institute's Ethics Committee of the Affiliated Hospital of Jining Medical University, Jining, China (approval number: 2022C210).

Funding

This study was supported by PhD Research Foundation of Affiliated Hospital of Jining Medical University (Grant NO. 2021-BS-006); 2022 key research and development program of Jining Science and Technology Bureau (policy guidance) (No. 2022YXNS031).

CRediT authorship contribution statement

Bo Li: Writing – original draft, Supervision, Funding acquisition, Data curation. **Ziyi Yang:** Writing – original draft, Validation, Software, Investigation, Formal analysis, Data curation. **Lulu Li:** Validation, Formal analysis, Data curation. **Yongxin Wang:** Visualization, Validation, Methodology. **Feng Jin:** Validation, Investigation, Data curation. **Lu Zhang:** Validation, Investigation, Data curation. **Youjing Zhang:** Writing – original draft, Visualization, Validation, Software, Investigation, Data curation.

Declaration of competing interest

The authors declare that they have no competing interests.

Data availability

The data that has been used is confidential.

Appendix A. Supplementary data

Supplementary data to this article can be found online at https://doi.org/10.1016/j.bbrep.2023.101603.

References

[1] A. Omuro, L.M. DeAngelis, Glioblastoma and other malignant gliomas: a clinical review, JAMA 310 (2013) 1842–1850.
[2] D.N. Louis, H. Ohgaki, O.D. Wiestler, W.K. Cavenee, P.C. Burger, A. Jouvet, B. W. Scheithauer, P. Kleihues, The 2007 WHO classification of tumours of the central nervous system, Acta Neuropathol. 114 (2007) 97–109.
[3] T.T. Lah, M. Novak, B. Breznik, Brain malignancies: glioblastoma and brain metastases, Semin. Cancer Biol. 60 (2020) 262–273.
[4] C.M. Jackson, J. Choi, M. Lim, Mechanisms of immunotherapy resistance: lessons from glioblastoma, Nat. Immunol. 20 (2019) 1100–1109.
[5] E. Lee, R.L. Yong, P. Paddison, J. Zhu, Comparison of glioblastoma (GBM) molecular classification methods, Semin. Cancer Biol. 53 (2018) 201–211.
[6] E. Fletcher-Sananikone, S. Kanji, N. Tomimatsu, L.F.M. Di Cristofaro, R. K. Kollipara, D. Saha, J.R. Floyd, P. Sung, R. Hromas, T.C. Burns, R. Kittler, A. A. Habib, B. Mukherjee, S. Burma, Elimination of radiation-induced senescence in the brain tumor microenvironment attenuates glioblastoma recurrence, Cancer Res. 81 (2021) 5935–5947.
[7] M. Alexovič, J. Sabo, R. Longuespée, Microproteomic sample preparation, Proteomics 21 (2021), e2000318.
[8] J. Chen, A. Balakrishnan-Renuka, N. Hagemann, C. Theiss, V. Chankiewitz, J. Chen, Q. Pu, K.S. Erdmann, B. Brand-Saberi, A novel interaction between ATOH8 and PPP3CB, Histochem. Cell Biol. 145 (2016) 5–16.
[9] H. Li, A. Rao, P.G. Hogan, Interaction of calcineurin with substrates and targeting proteins, Trends Cell Biol. 21 (2011) 91–103.
[10] A. Stern, E. Privman, M. Rasis, S. Lavi, T. Pupko, Evolution of the metazoan protein phosphatase 2C superfamily, J. Mol. Evol. 64 (2007) 61–70.
[11] L. Chen, Q. He, Y. Liu, Y. Wu, D. Ni, J. Liu, Y. Hu, Y. Gu, Y. Xie, Q. Zhou, Q. Li, PPP3CB inhibits migration of G401 cells via regulating epithelial-to-mesenchymal transition and promotes G401 cells growth, Int. J. Mol. Sci. 20 (2019) 275.
[12] I. Shakhova, Y. Li, F. Yu, Y. Kaneko, Y. Nakamura, M. Ohira, H. Izumi, T. Mae, S. R. Varfolomeeva, A.G. Rumyantsev, A. Nakagawara, PPP3CB contributes to poor prognosis through activating nuclear factor of activated T-cells signaling in neuroblastoma, Mol. Carcinog. 58 (2019) 426–435.
[13] L. Luo, Z. Zhang, N. Qiu, L. Ling, X. Jia, Y. Song, H. Li, J. Li, H. Lyu, H. Liu, Z. He, B. Liu, G. Zheng, Disruption of FOXO3a-miRNA feedback inhibition of IGF2/IGF-1R/IRS1 signaling confers Herceptin resistance in HER2-positive breast cancer, Nat. Commun. 12 (2021) 2699.
[14] W. Lou, B. Ding, L. Xu, W. Fan, Construction of potential glioblastoma multiforme-related miRNA-mRNA regulatory network, Front. Mol. Neurosci. 12 (2019) 66.
[15] J.N. Weinstein, E.A. Collisson, G.B. Mills, K.R. Shaw, B.A. Ozenberger, K. Ellrott, I. Shmulevich, C. Sander, J.M. Stuart, The cancer genome Atlas pan-cancer analysis project, Nat. Genet. 45 (2013) 1113–1120.
[16] Z. Zhao, K.N. Zhang, Q. Wang, G. Li, F. Zeng, Y. Zhang, F. Wu, R. Chai, Z. Wang, C. Zhang, W. Zhang, Z. Bao, T. Jiang, Chinese glioma genome Atlas (CGGA): a comprehensive resource with functional genomic data from Chinese glioma patients, Dev. Reprod. Biol. 19 (2021) 1–12.
[17] The genotype-tissue expression (GTEx) project, Nat. Genet. 45 (2013) 580–585.
[18] Z. Tang, C. Li, B. Kang, G. Gao, C. Li, Z. Zhang, GEPIA: a web server for cancer and normal gene expression profiling and interactive analyses, Nucleic Acids Res. 45 (2017) W98–w102.
[19] J. Wu, H. Zhang, L. Li, M. Hu, L. Chen, B. Xu, Q. Song, A nomogram for predicting overall survival in patients with low-grade endometrial stromal sarcoma: a population-based analysis, Cancer Commun. 40 (2020) 301–312.
[20] A. Subramanian, P. Tamayo, V.K. Mootha, S. Mukherjee, B.L. Ebert, M.A. Gillette, A. Paulovich, S.L. Pomeroy, T.R. Golub, E.S. Lander, J.P. Mesirov, Gene set enrichment analysis: a knowledge-based approach for interpreting genome-wide expression profiles, Proc. Natl. Acad. Sci. U. S. A. 102 (2005) 15545–15550.
[21] R. Zhou, J. Zhang, D. Zeng, H. Sun, X. Rong, M. Shi, J. Bin, Y. Liao, W. Liao, Immune cell infiltration as a biomarker for the diagnosis and prognosis of stage I-III colon cancer, Cancer Immunol. Immunother. 68 (2019) 433–442.
[22] B. Ricciuti, X. Wang, J.V. Alessi, H. Rizvi, N.R. Mahadevan, Y.Y. Li, A. Polio, J. Lindsay, R. Umeton, R. Sinha, N.I. Vokes, G. Recondo, G. Lamberti, M. Lawrence, V.R. Vaz, G.C. Leonardi, A.J. Plodkowski, H. Gupta, A.D. Cherniack, M. Y. Tolstorukov, B. Sharma, K.D. Felt, J.F. Gainor, A. Ravi, G. Getz, K.A. Schalper, B. Henick, P. Forde, V. Anagnostou, P.A. Jänne, E.M. Van Allen, M. Nishino, L. M. Sholl, D.C. Christiani, X. Lin, S.J. Rodig, M.D. Hellmann, M.M. Awad, Association of high tumor mutation burden in non-small cell lung cancers with increased immune infiltration and improved clinical outcomes of PD-L1 blockade across PD-L1 expression levels, JAMA Oncol. 8 (2022) 1160–1168.
[23] K. Liu, J.J. Cui, Y. Zhan, Q.Y. Ouyang, Q.S. Lu, D.H. Yang, X.P. Li, J.Y. Yin, Reprogramming the tumor microenvironment by genome editing for precision cancer therapy, Mol. Cancer 21 (2022) 98.
[24] T. Tang, X. Huang, G. Zhang, Z. Hong, X. Bai, T. Liang, Advantages of targeting the tumor immune microenvironment over blocking immune checkpoint in cancer immunotherapy, Signal Transduct. Targeted Ther. 6 (2021) 72.
[25] J. Hang, S.Y. Lau, R. Yin, L. Zhu, S. Zhou, X. Yuan, L. Wu, The role of phosphoprotein phosphatases catalytic subunit genes in pancreatic cancer, Biosci. Rep. 41 (2021).
[26] A. Nolze, C. Köhler, S. Ruhs, K. Quarch, N. Strätz, M. Gekle, C. Grossmann, Calcineurin (PPP3CB) regulates angiotensin II-dependent vascular remodelling by potentiating EGFR signalling in mice, Acta Physiol. 233 (2021), e13715.
[27] J. Wu, C. Zheng, X. Wang, S. Yun, Y. Zhao, L. Liu, Y. Lu, Y. Ye, X. Zhu, C. Zhang, S. Shi, Z. Liu, MicroRNA-30 family members regulate calcium/calcineurin signaling in podocytes, J. Clin. Invest. 125 (2015) 4091–4106.
[28] C.M. Liu, C.S. Fann, C.Y. Chen, Y.L. Liu, Y.J. Oyang, W.C. Yang, C.C. Chang, C. C. Wen, W.J. Chen, T.J. Hwang, M.H. Hsieh, C.C. Liu, S.V. Faraone, M.T. Tsuang, H.G. Hwu, ANXA7, PPP3CB, DNAJC9, and ZMYND17 genes at chromosome 10q22 associated with the subgroup of schizophrenia with deficits in attention and executive function, Biol. Psychiatr. 70 (2011) 51–58.
[29] G.P. Dotto, Calcineurin signaling as a negative determinant of keratinocyte cancer stem cell potential and carcinogenesis, Cancer Res. 71 (2011) 2029–2033.
[30] C. Aggarwal, R. Ben-Shachar, Y. Gao, S.W. Hyun, Z. Rivers, C. Epstein, K. Kaneva, C. Sangli, H. Nimeiri, J. Patel, Assessment of tumor mutational burden and outcomes in patients with diverse advanced cancers treated with immunotherapy, JAMA Netw. Open 6 (2023), e2311181.
[31] M. Gromeier, M.C. Brown, G. Zhang, X. Lin, Y. Chen, Z. Wei, N. Beaubier, H. Yan, Y. He, A. Desjardins, J.E. Herndon 2nd, F.S. Varn, R.G. Verhaak, J. Zhao, D. P. Bolognesi, A.H. Friedman, H.S. Friedman, F. McSherry, A.M. Muscat, E.S. Lipp, S.K. Nair, M. Khasraw, K.B. Peters, D. Randazzo, J.H. Sampson, R.E. McLendon, D. D. Bigner, D.M. Ashley, Very low mutation burden is a feature of inflamed recurrent glioblastomas responsive to cancer immunotherapy, Nat. Commun. 12 (2021) 352.
[32] P. Chen, W.H. Hsu, A. Chang, Z. Tan, Z. Lan, A. Zhou, D.J. Spring, F.F. Lang, Y. A. Wang, R.A. DePinho, Circadian regulator CLOCK recruits immune-suppressive microglia into the GBM tumor microenvironment, Cancer Discov. 10 (2020) 371–381.
[33] M.S. Pavlyukov, H. Yu, S. Bastola, M. Minata, V.O. Shender, Y. Lee, S. Zhang, J. Wang, S. Komarova, J. Wang, S. Yamaguchi, H.A. Alsheikh, J. Shi, D. Chen, A. Mohyeldin, S.H. Kim, Y.J. Shin, K. Anufrieva, E.G. Evtushenko, N.V. Antipova, G.P. Arapidi, V. Govorun, N.B. Pestov, M.I. Shakhparonov, L.J. Lee, D.H. Nam, I. Nakano, Apoptotic cell-derived extracellular vesicles promote malignancy of glioblastoma via intercellular transfer of splicing factors, Cancer Cell 34 (2018) 119–135.e10.